# INTERFEROMETRIC PROFILOMETRY OF A METAL SURFACE BEARING A DIELECTRIC COATING

by

Maurice Bruce Stewart

1955

## Abstract

The practicability of using multiple-beam interferometry to study the surfaces of metals with oxide coatings is demonstrated in the case of aluminum. Topographical variations ranging from a tenth of a micron to one and one half microns in depth can be measured by means of the fringes of equal chromatic order. Although the presence of the oxide broadens the fringes, it does not distort the profile provided that the interferometer spacing is made much greater than the oxide thickness.

Large local variations in oxide thickness observed show that the oxide does not contour the substratum. In this respect, the oxide which forms naturally on a surface differs from a thin evaporated film.

(F)

THE UNIVERSITY OF ALBERTA

# INTERFEROMETRIC PROFILOMETRY OF A METAL SURFACE BEARING A DIELECTRIC COATING

A DISSERTATION

SUBMITTED TO THE SCHOOL OF GRADUATE STUDIES

IN PARTIAL FULFILMENT OF THE REQUIREMENTS FOR THE DEGREE

OF MASTER OF SCIENCE

FACULTY OF ARTS AND SCIENCE

DEPARTMENT OF PHYSICS

by

MAURICE BRUCE STEWART

EDMONTON, ALBERTA

September 1955

I wish to acknowledge the grants made to aid this research by the National Research Council and by the Defence Research Board.

I wish to thank Dr. J.H. Harrold for suggesting this project to me, and for his advice and encouragement during its completion.

The help of Mr. F. Gleave and his assistants in solving many technical problems is gratefully acknowledged.

I also wish to thank the other members of the Physics Department who gave freely of their knowledge.

# Contents

## List of Tables

## List of Figures

## I. Introduction

The use of multiple-beam interferometry to study the topography of metal surfaces was suggested by Chalmers and Hoare[1] in 1938. The elegantly simple method consists of observing the interference fringes which arise between a partially reflecting optical flat and the surface of the specimen being examined. The technique has two complementary aspects, the one using white light illumination, giving rise to a profile of a line along the specimen, the other, employing monochromatic light, producing a contour map of an area of the specimen. The method has been developed and refined by Tolansky[2] in applications to both opaque and transparent specimens.

---

1. B. Chalmers and W.E. Hoare, Nature 141, 475 (1938).

2. S. Tolansky, Multiple-Beam Interferometry of Surfaces and Films (Clarendon Press, Oxford, 1948).

## II. Theory

### a. Monochromatic Illumination

Let $\rho_i$ and $\sigma_i$ be the reflectivity and transmissivity of the $i^{th}$ surface. $\epsilon_i$ is the phase change upon reflection at the $i^{th}$ surface for a beam passing in the direction from surface I (Fig. 1) to surface II. $\epsilon_i'$ is the phase change for a beam travelling in the opposite direction.

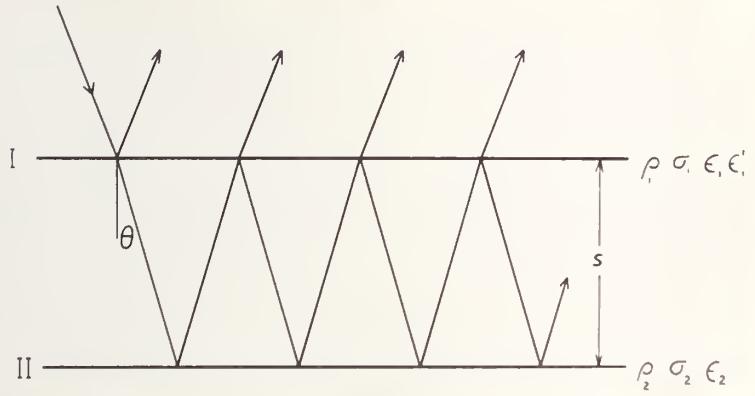


Fig. 1. Interference arising from two parallel plane surfaces.

If a beam of unit amplitude strikes surface I, the amplitude of the first reflected beam is $\rho_1^{\frac{1}{2}} e^{-i\epsilon_1}$. Each time the beam passes from one surface to the other, a phase difference of $\delta = \frac{2\pi}{\mu\lambda} s \cos\theta$ is added to the beam, where $\mu$ is the index of refraction of the medium between surfaces I and II, and $\lambda$ is the wavelength of the light.

So the total reflected amplitude is

$$A = \rho_1^{\frac{1}{2}} e^{-i\epsilon_1} + \sum_{n=1}^{\infty} \sigma_1 e^{-i\delta} \left[\rho_2^{\frac{1}{2}} e^{i(\delta-\epsilon_2)}\right]^n \left[\rho_1^{\frac{1}{2}} e^{i(\delta-\epsilon_1')}\right]^{n-1} \qquad (1)$$

$$= \rho_1^{\frac{1}{2}} e^{-i\epsilon_1} + \frac{\sigma_1 \rho_2^{\frac{1}{2}} e^{i2\delta}\, e^{-i\epsilon_2}}{1 + (\rho_1\rho_2)^{\frac{1}{2}} e^{i2\delta}\, e^{-i(\epsilon_1'+\epsilon_2)}} \qquad (2)$$

The reflected intensity is

$$AA^* = \rho_1 + \sigma_1 \frac{\sigma_1\rho_2 - 2(\rho_1\rho_2)^{\frac{1}{2}}\left[\cos(2\delta+\epsilon_1-\epsilon_2) + \cos(\epsilon_1'-\epsilon_1)\right]}{1 - 2(\rho_1\rho_2)^{\frac{1}{2}}\cos(2\delta-\epsilon_1'-\epsilon_2) + \rho_1\rho_2} \qquad (3)$$

Dark fringes will occur when $\frac{dAA^*}{d\delta} = 0$. It is obvious from equation (3) that if $\delta_0$ is a solution of $\frac{dAA^*}{d\delta} = 0$, so is $\delta_0 + m\pi$, where m is an integer. So there is some distance $s_0$, say, for which a dark fringe occurs when

$$\delta_0 = \frac{2\pi}{\mu\lambda} s_0 \cos\theta \quad \Big| \quad -1 \qquad (4)$$

and some other distance, $s_m$, for which

$$\delta_m = \frac{2\pi}{\mu\lambda} s_m \cos\theta \quad \Big| \quad 1 \qquad (5)$$

Whence, by the indicated subtraction, it is seen that

$$s_m - s_o = \frac{m\mu\lambda}{2\cos\theta} \tag{6}$$

Thus for normal illumination, the fringes contour at intervals of $\frac{\mu\lambda}{2}$.

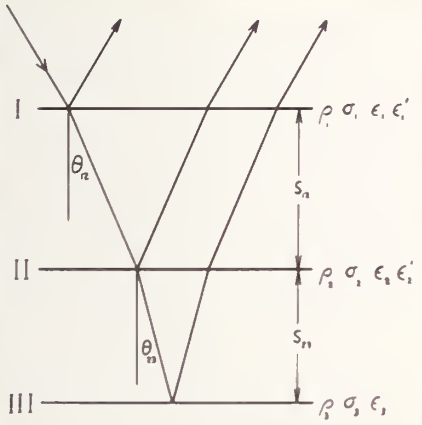


Fig. 2. Interference arising from three parallel plane surfaces.

When the surface under examination is aluminum, there is a coating of aluminum oxide on the aluminum surface. So interference arising from the presence of three surfaces must be considered (Fig. 2). The beam of amplitude $\sigma_1^{\frac{1}{2}}$ which passes through surface I may be regarded as composite. The various components are reflected an odd number of times and then re-emerge from surface I. If $u_m$ is a Fibonacci

number[3], it may be shown that $u_{2n}$ components emerge after $2n-1$ reflections[4]. Since $u_{30} = 1{,}346{,}069$, an exact treatment by generalizing the two surface case is almost certainly bound to be extremely unwieldy. Mooney[5] has obtained a solution to the problem by boundary value methods.

However, the more complicated three surface case may be regarded as a modification to the simpler two surface case, which has been treated exactly, above. If $\mu_{12}$ is the index of refraction of the medium between surfaces I and II, and similarly for $\mu_{23}$, then the reflectivity of surface II is[6]

$$\rho_2 = \left( \frac{\mu_{12} - \mu_{23}}{\mu_{12} + \mu_{23}} \right)^2 \qquad (7)$$

In the practical case, $\mu_{12}$ is the index of refraction of air, while $\mu_{23}$ is that for aluminum oxide. If $\mu_{23}$ is taken to be 1.765[7], then $\rho_2$ is 0.083.

---

3. G.H. Hardy and E.M. Wright, An Introduction to the Theory of Numbers (Clarendon Press, Oxford, 1938), p. 147.

4. Personal communication from J.R. Trollope, to whom I am indebted for an ingenious proof of this proposition.

5. R.L. Mooney, J. Opt. Soc. Am. 35, 574 (1945).

6. J.C. Slater and N.H. Frank, Electromagnetism (McGraw-Hill Book Company, Inc., New York, 1947), p. 120.

7. Handbook of Chemistry and Physics (Chemical Rubber Publishing Company, Cleveland, 1953), thirty-fifth edition, p. 468, but cf. p. 2648.

So most of the energy passes through surface II and is reflected to and fro between surfaces I and III. These beams are the dominant beams and give rise to a fringe pattern similar to that in the two surface case.

For a given number of reflections, the dominant beam, which is never reflected from surface II, evidently passes over the longest path. A beam which is reflected once at surface II traverses the next longest path, and so on. However, due to the low reflectivity of surface II, beams travelling shorter and shorter paths carry less and less of the total energy. Since the sharpness of the fringes depends upon a large number of beams of similar phase interfering with one another, the effect of the reflections at surface II is to broaden the fringes.

So in the three surface case, the fringes still contour at intervals of $\frac{\mu\lambda}{2}$. However, $\mu$ is now an average such that

$$\mu(s_{12} + s_{23}) = \mu_{12}s_{12} + \mu_{23}s_{23} \qquad (8)$$

It is a consequence of the binomial theorem that

$$\mu = \mu\left\{1 + \left(\frac{\mu_{23}}{\mu_{12}} - 1\right)\frac{s_{23}}{s_{12}} - \left(\frac{\mu_{23}}{\mu_{12}} - 1\right)\left(\frac{s_{23}}{s_{12}}\right)^2 + \cdots\right\} \qquad (9)$$

For aluminum, $\frac{\mu_{23}}{\mu_{12}} - 1$ is never greater than 0.765. $s_{23}$ is the thickness of the aluminum oxide film, which if formed under ordinary atmospheric conditions is, according to Kubaschewski and Hopkins[8], about five millimicrons thick. In these experiments, $s_{12}$ is about ten microns. So in the ordinary case, it is seen from equation (9) that $\mu = 1.00034\,\mu_{12}$. Oxide thicknesses on heat treated aluminum specimens have been discussed by Smeltzer[9], who cites thicknesses the order of one tenth of a micron for a specimen maintained at 600° C for twenty-four hours. So even for this extreme case, it appears from equation (9) that $\mu = 1.0077\,\mu_{12}$.

b. White Light Illumination

If white light is allowed to fall on surface I (Fig. 1), fringes of equal chromatic order arise. The condition for destructive interference among the successive reflected beams is that

$$\frac{2\pi}{\mu\lambda_n} 2s + \epsilon_1' + \epsilon_2 = (2n+1)\pi \qquad (10)$$

---

8. O. Kubaschewski and B.E. Hopkins, Oxidation of Metals and Alloys (Butterworth Scientific Publications, London, 1953), p. 131.

9. W.W. Smeltzer, Aluminium Laboratories Limited Report No. K-RR-450-54-28 (Kingston, 1954), p. 19 - 29.

In this equation, n is some integer. In general, if s is not too small and all wavelengths of light are available, there will exist at least one value of n which satisfies equation (10). In the actual experiments performed, s was always sufficiently large that there were many integers satisfying the equation.

In textbook treatments of interference in thin films, the phase changes, $\epsilon_1'$ at the upper surface (a dielectric in these experiments) and $\epsilon_2$ at the lower surface (the oxidized aluminum surface), are assigned definite values of either 0 or an advance or retardation of phase of $\pi$, and $\frac{2\pi}{\mu\lambda_n} 2s$ is then either an odd or an even integral multiple of $\pi$. In order that the index numbers for adjacent fringes may differ by unity, in all cases, even those in which two might seem a more natural difference, the interference minimum is called the $n^{th}$ interference fringe.

The present case is not so simple as the textbook case since the total phase change is not known. The phase change at the metal surface, $\epsilon_2$, is not $\pi$ unless the light is normally incident, which cannot be the case in the presence of interesting topographical variations. Furthermore, in these experiments the surface is not that of a pure metal, but rather that of a metal overlaid by oxide. If $\epsilon \equiv \epsilon_1' + \epsilon_2$, then

equation (10) may be rewritten as

$$\frac{2\pi}{\mu\lambda_n} 2s = (2n' + 1)\pi \qquad (10')$$

where $n' \equiv n - \frac{\epsilon}{2\pi}$ and is in general not integral. The phrase, "$n^{th}$ fringe," is thus not an altogether happy one, but, alternatively, equation (10) might be rewritten as

$$\frac{2\pi}{\mu\lambda_n} 2s' = (2n + 1)\pi \qquad (10'')$$

where $s' \equiv s + \epsilon \frac{\mu\lambda_n}{2\pi}$ , which is of course not the actual distance between the reflecting surfaces.

Equation (10) cannot be used, by itself, to find s because n and $\epsilon$ are also unknowns in it. To solve this problem, the wavelengths, $\lambda_{n+m}$ , m = 1, 2, ..., of fringes adjacent to $\lambda_n$ are also measured. For these it is clear that

$$\frac{2\pi}{\mu\lambda_{n+m}} 2s + \epsilon = [2(n+m) + 1]\pi \qquad (11)$$

Again, $\epsilon$ may be absorbed into either n+m or s, but since the former procedure will result in the same n' as in equation (10') whereas the latter procedure will not lead to s' but rather to $s'' \equiv s + \epsilon \frac{\mu\lambda_{n+m}}{2\pi}$, the former procedure is adopted,

yielding

$$\frac{2\pi}{\mu\lambda_{n+m}} 2s = [2(n'+m)+1]\pi \qquad (11')$$

The identity of the n' obtained from equation (11') with that of equation (10') is assured only if $\epsilon$ does not change with the wavelength change of $\lambda_n$ to $\lambda_{n+m}$. In these experiments, $\lambda_n$ was about 5000A and $\lambda_{n+m}$ was not more than 500A less than $\lambda_n$ for the range of m employed. Since this spectral region is not near any absorption bands of the reflecting materials, regarding $\epsilon$ as constant, albeit unknown, will introduce only a negligible error into the calculation of s at a given position on a profile.

Fortunately, because of the form of equations (10) and (11), the non-integral fringe index numbers do not actually appear. For if equation (10) is subtracted from equation (11) it is found that

$$\frac{2\pi}{\mu}\left(\frac{1}{\lambda_{n+m}} - \frac{1}{\lambda_n}\right) 2s = 2m\pi \qquad (12)$$

in which neither n nor $\epsilon$ appears. If $r \equiv \frac{\lambda_n}{\lambda_{n+m}}$, further algebraic manipulation reveals that

$$s = \frac{m}{r-1} \frac{\mu\lambda_n}{2} \qquad (13)$$

Thus s may be found by determining the wavelengths of successive fringes, thence r, and thence $\frac{m}{r-1}$. It follows from the definition of r and equation (10') that

$$\frac{m}{r-1} = n' + \frac{1}{2} \tag{14}$$

If in the experiments, the phase changes are those for clean surfaces at normal incidence, there will be two phase changes of $\pi$ and $\frac{m}{r-1}$ will be half-integral.

The work of Scott[10] shows that $\mu_{23}$ may be taken to be 1.765, the index of refraction of aluminum oxide in bulk. Then, to the first order in $\frac{s_{23}}{s_{12}}$, equation (9) becomes

$$\mu = 1 + 0.765 \frac{s_{23}}{s_{12}} \tag{15}$$

provided that air fills the gap between the flat and the oxide coating. So that, if the profile is constructed on the basis of

$$s = \frac{m}{r-1} \frac{\lambda_n}{2} \tag{16}$$

there will be a fractional error of $0.765 \frac{s_{23}}{s_{12}}$ introduced.

---

10. G.D. Scott, J. Opt. Soc. Am. 45, 179 (1955).

Even under the extreme conditions of prolonged heating discussed on page seven above, this fractional error is only 0.8%. This error will be subject to minor variations if the oxide is not equally aggregated over the metal surface, so that its refractive index varies from the bulk index from place to place. This effect, as well as that of variable oxide thickness, may cause local variations in the breadth of the fringes.

This systematic error, it should be noted, is calculated on the assumption that there is an air gap between the flat and the surface being examined. If a liquid immersion method is employed, the numerical values of the various quantities may not be the same.

## III. Precision of the Measurements

As the first step in computing the profile, $\frac{m}{r-1}$ was found (Table I).

Table I. Calculation of $\frac{m}{r-1}$ for section GG (Fig. 10) at 300 microns†.

| m | $\lambda_{A}^{n+m}$ | r − 1 | $\frac{m}{r-1}$ |
|---|---|---|---|
| 0 | 5105 ± 10* | | |
| 1 | 5050 ± 10 | 0.01089 ± .00398 | 91.83 ± 26.13 |
| 2 | 4995 ± 10 | 0.02202 ± .00405 | 90.82 ± 16.70 |
| 3 | 4940 ± 10 | 0.03341 ± .00412 | 89.79 ± 11.07 |
| 4 | 4890 ± 10 | 0.04397 ± .00418 | 90.97 ± 8.65 |
| 5 | 4845 ± 10 | 0.05366 ± .00424 | 93.18 ± 7.36 |
| 6 | 4790 ± 10 | 0.06576 ± .00431 | 91.24 ± 5.98 |
| 7 | 4740 ± 10 | 0.07701 ± .00438 | 90.89 ± 5.17 |
| 8 | 4695 ± 10 | 0.08733 ± .00445 | 91.61 ± 4.67 |
| 9 | 4650 ± 10 | 0.09785 ± .00451 | 91.98 ± 4.24 |
| 10 | 4605 ± 10 | 0.10858 ± .00458 | 92.10 ± 3.89 |

The values of $\frac{m}{r-1}$ have strikingly large tolerances, but are in fact closely clustered. Some average of these ten values must be used in equation (16). If each of the tabular entries is given equal weight, the average is found to be 91.44 with a standard deviation of 0.87, or 0.95%. This is the average to be used if, despite the tolerances, the close clustering is regarded as significant. In these experiments, the close

---

† See page 21.

* 5105 ± 10 means that $\lambda$ almost certainly lies between 5095 and 5115.

clustering was always encountered, and it seems unlikely that it is only fortuitous. However, if the ten values of $\frac{m}{r-1}$ are averaged so as to give the most weight to the values with the smallest tolerances, the average is found to be 91.66 with a standard deviation of 0.94, or 1.0%. Since in practice, both averages have standard deviations of about one percent, there seems no reason for not choosing the simple average, which is much easier to compute.

The classic "half-table" method for obtaining numbers which bear a large ratio to the tolerances involved would not be strictly relevant in this case. It would indeed be possible to calculate, with a range of values of $\lambda_n$ for ten successive fringes, say, a single value of $\frac{m}{r-1}$ with a small tolerance by using $m = 10$ only. In this way ten determinations of s could be obtained, although the changing value of $\lambda_n$ would mean that each determination employed a different unit of measurement, but the total wavelength range would have to be doubled, thereby casting doubt on the validity of the assumption of constancy in the phase changes. The half-table method is, thus, unsuitable.

The tolerances in the wavelength measurements, ten parts in five thousand, when considered together with the 0.8% systematic error in neglecting the index of refraction of the oxide-air combination, and the one percent treated directly above, make a total tolerance of about two percent in the profile distances.

## IV. Experimental Technique

### a. Monochromatic Fringes

The schematic diagram (Fig. 3) shows how the monochromatic fringes were observed. In order to minimize undesirable continuous bands in the spectrum, a low pressure mercury arc was employed. The desired line of the mercury spectrum, usually the green line, was selected by means of a Wratten filter. The light was then directed into the vertical illuminator of the microscope by a condensing lens.

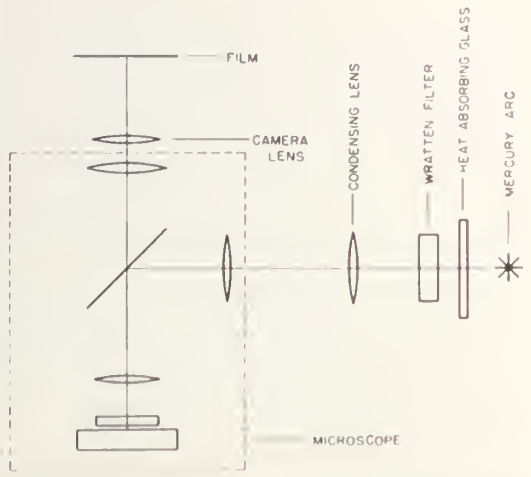


Fig. 3. Arrangement for observing monochromatic interference fringes. (Not to scale.)

By adjustment of this lens, a parallel beam of light was directed normally onto the specimen. Fig. 4 gives the details of the interferometer itself. The specimen was simply placed on the stage of a metallurgical microscope

and an optical flat laid on the specimen. The optical flat was coated with multi-layer dielectric materials chosen to produce suitable reflectivities. A photographic record of the fringes was made by placing a camera over the eyepiece of the microscope. Coated lenses of varying focal lengths were used in the camera to enable the magnification on the film to be altered.

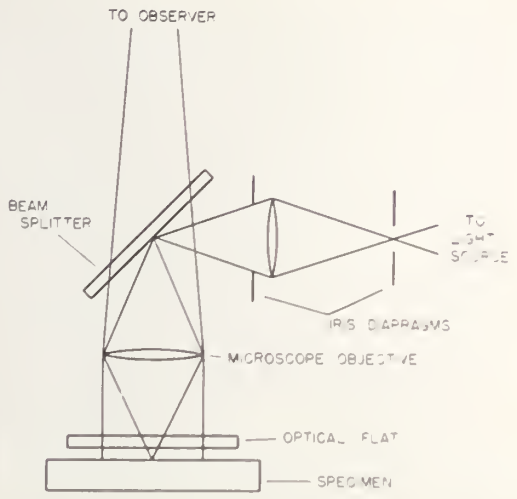


Fig. 4. The interferometer, consisting of a microscope with a vertical illuminator, and an optical flat. (Not to scale.)

b. Fringes of Equal Chromatic Order

To produce fringes of equal chromatic order the illumination system was similar to that for the monochromatic case except that a white light arc replaced the mercury arc and filter combination (Fig. 5). Also, the eyepiece was

removed from the microscope and the objective used to project an image of the specimen onto the slit of a constant deviation spectroscope by means of a reflecting prism. The resulting fringes were recorded photographically.

To provide a wavelength scale for the fringes of equal chromatic order, light from an iron arc was directed onto the edges of the slit of the spectroscope. This slit was surrounded by a white cardboard screen. A photograph of this screen showed the position of the line profiled on the specimen.

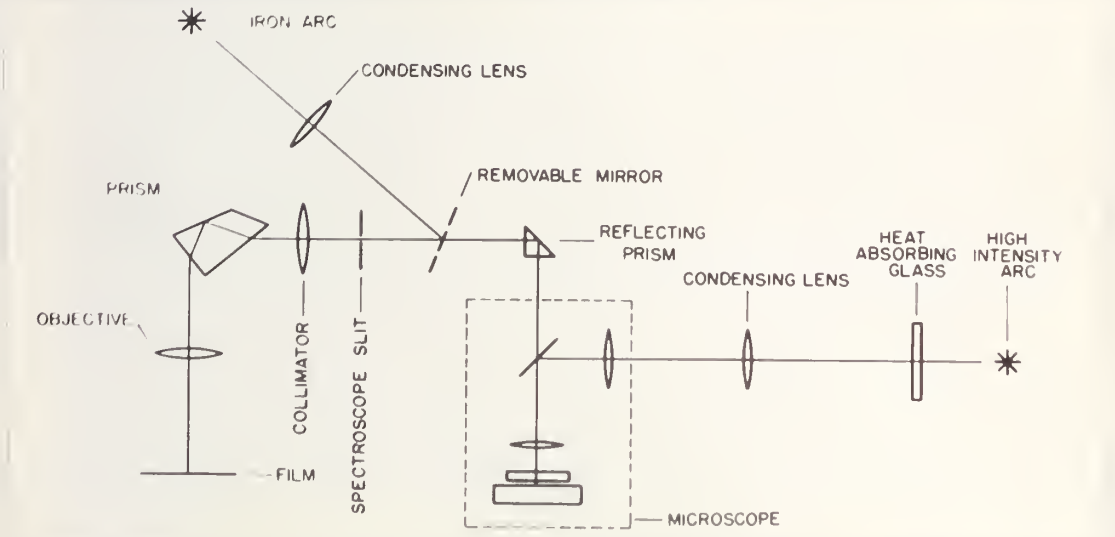


Fig. 5. Arrangement for observing fringes of equal chromatic order. (Not to scale.)

## V. Experimental Results

Fig. 6 shows the appearance of a small portion of the surface of a single aluminum crystal which has been etched after electropolishing. This region is crossed by a line

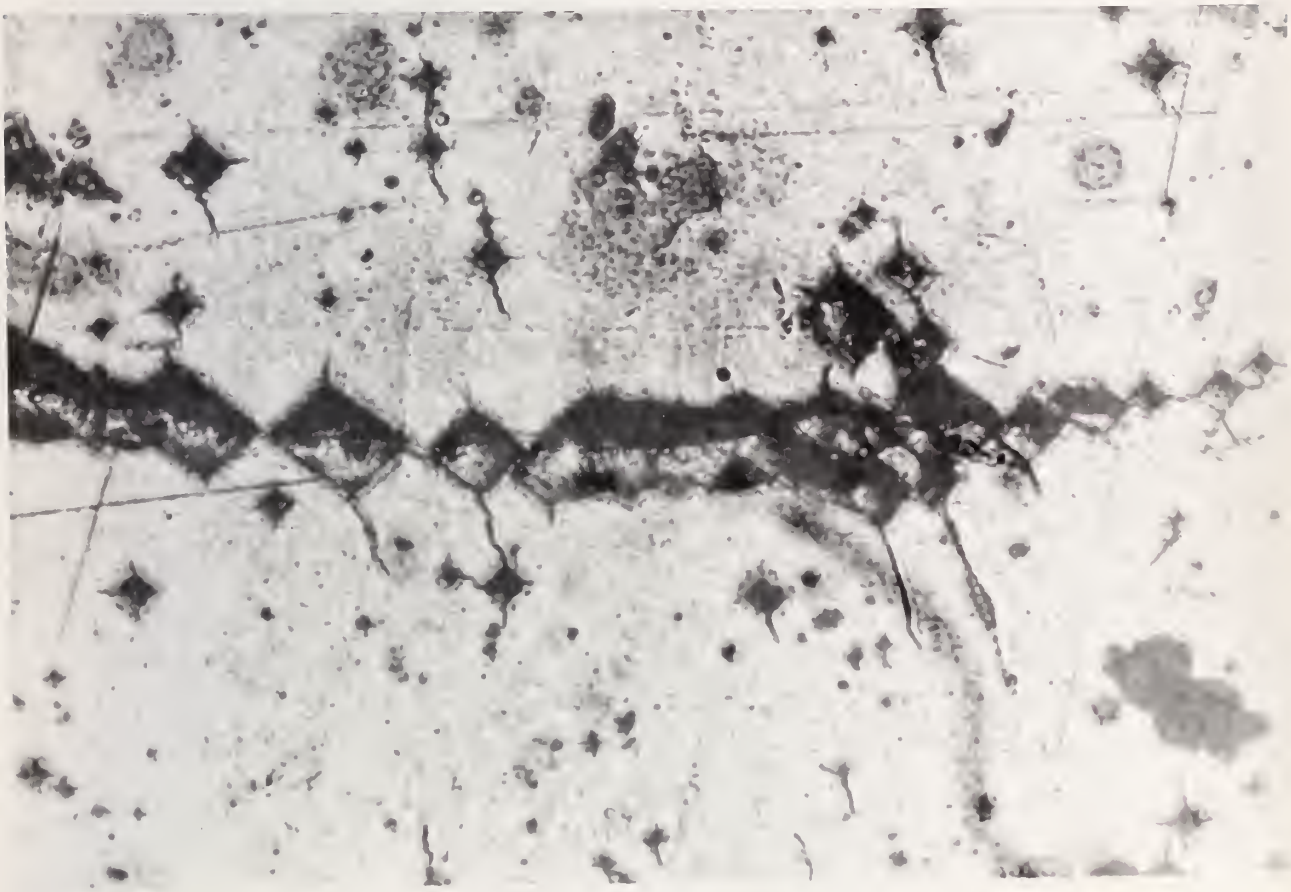

Fig. 6. A simple photomicrograph of a region (450$\mu$ by 300$\mu$) of a single aluminum crystal.

of features, which will subsequently be identified as etch pits. Another, less clearly defined, line of pits crosses the first

line at an angle of about forty-five degrees. The bottoms of the pits in the principal line are half-obscured by some matter of low reflectivity.

Fig. 7, an interferometric contour map of the same region, shows that this contaminating material also masked half of the fringe pattern in each of the pits in the principal line. The fringes, especially outside the pits, are seen to vary

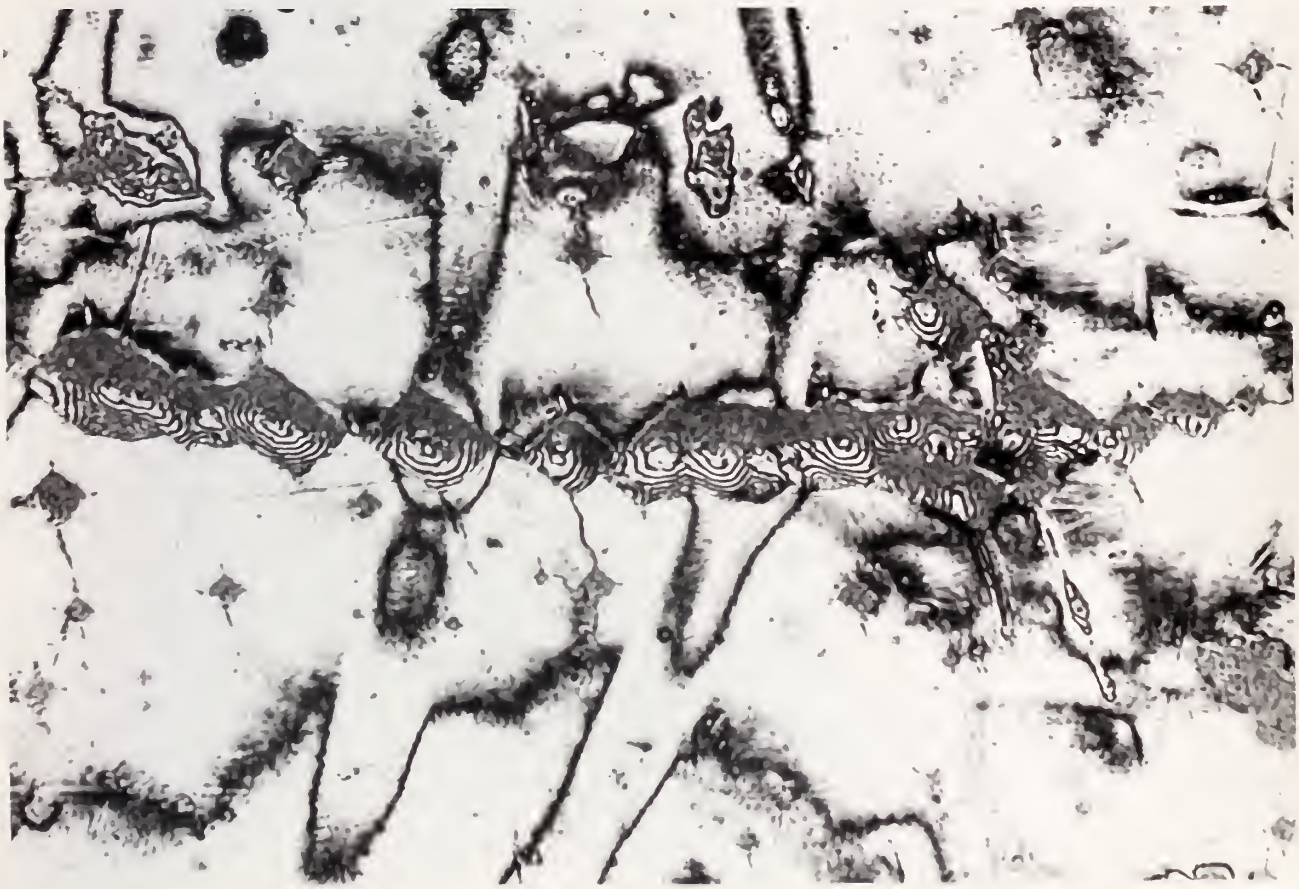

Fig. 7. An interferometric contour map of the same region shown in Fig. 6. (Contour interval 0.273$\mu$).

considerably in width. As will be seen, this is evidence of

variations in the thickness of the oxide coating.

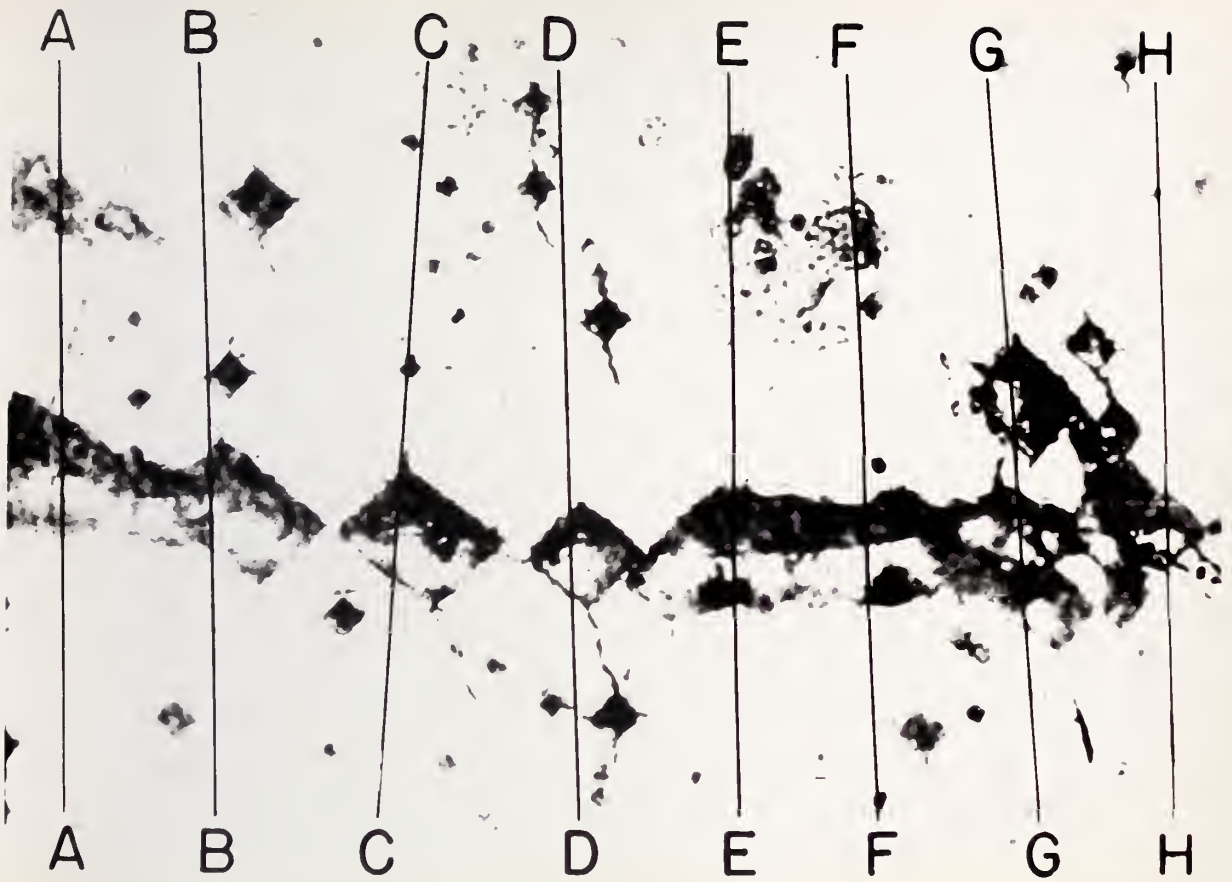


Fig. 8. Key to the profiles of the region shown in Fig. 6.

From Fig. 7 alone, it is not possible to determine whether the features are actually pits. This difficulty is overcome by use of the profiling technique involving fringes of equal chromatic order. The region of Fig. 6 was crossed by eight profile lines (Fig. 8). The fringe patterns themselves give a qualitative picture of the profiles (Figs. 9 and 10), for

clearly a shift to the red corresponds to a descent of the aluminum surface away from the optical flat. The band of fringes in Figs. 9 and 10 corresponds to a line 380 $\mu$ long on the specimen. Points along this profile line may be designated by giving their distance from the top of the band when the red end of the spectrum is at the right, e.g. in the caption of Table I (p. 13). Fig. 11 shows the complete set

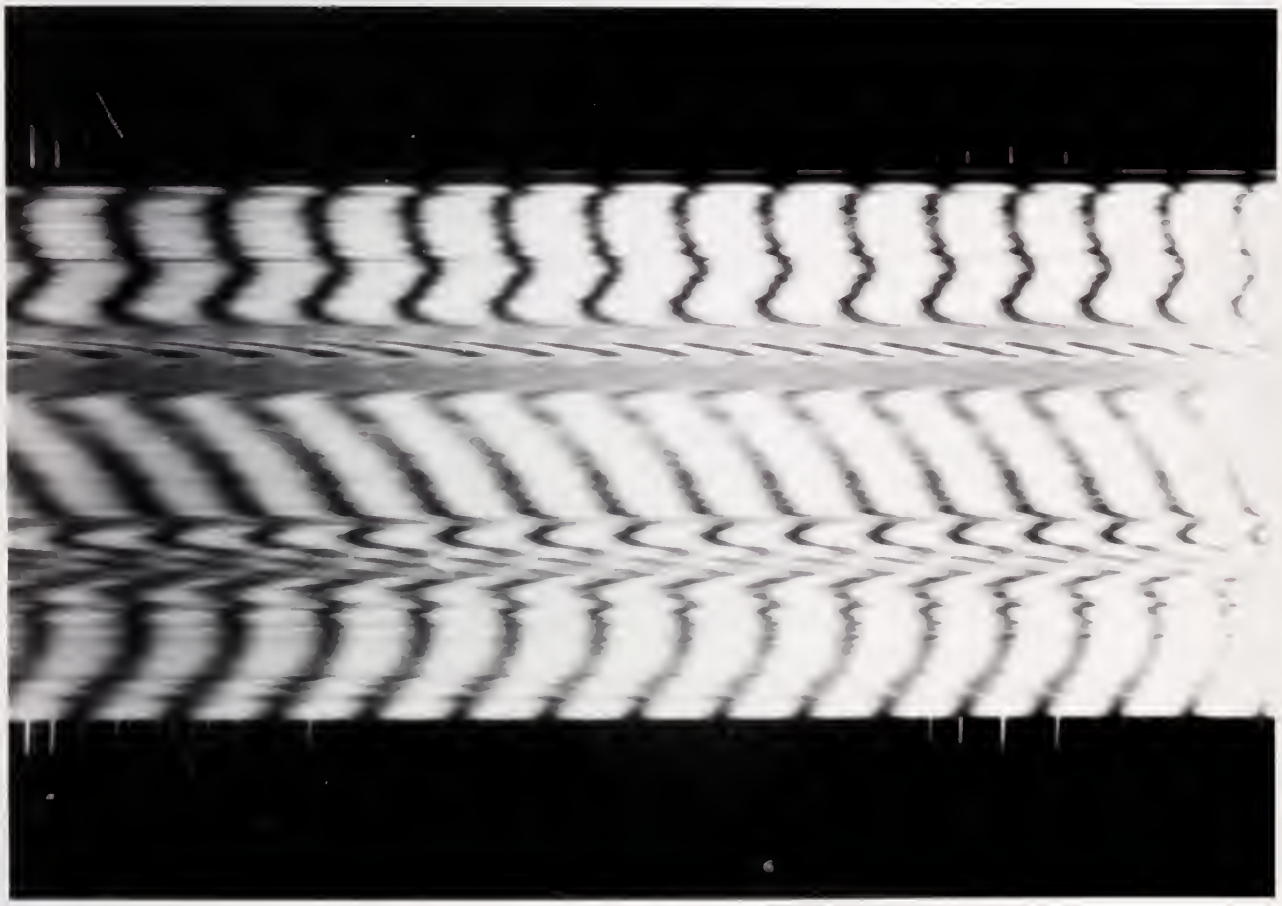

Fig. 9. Fringes of equal chromatic order.
Section FF as in Fig. 8.

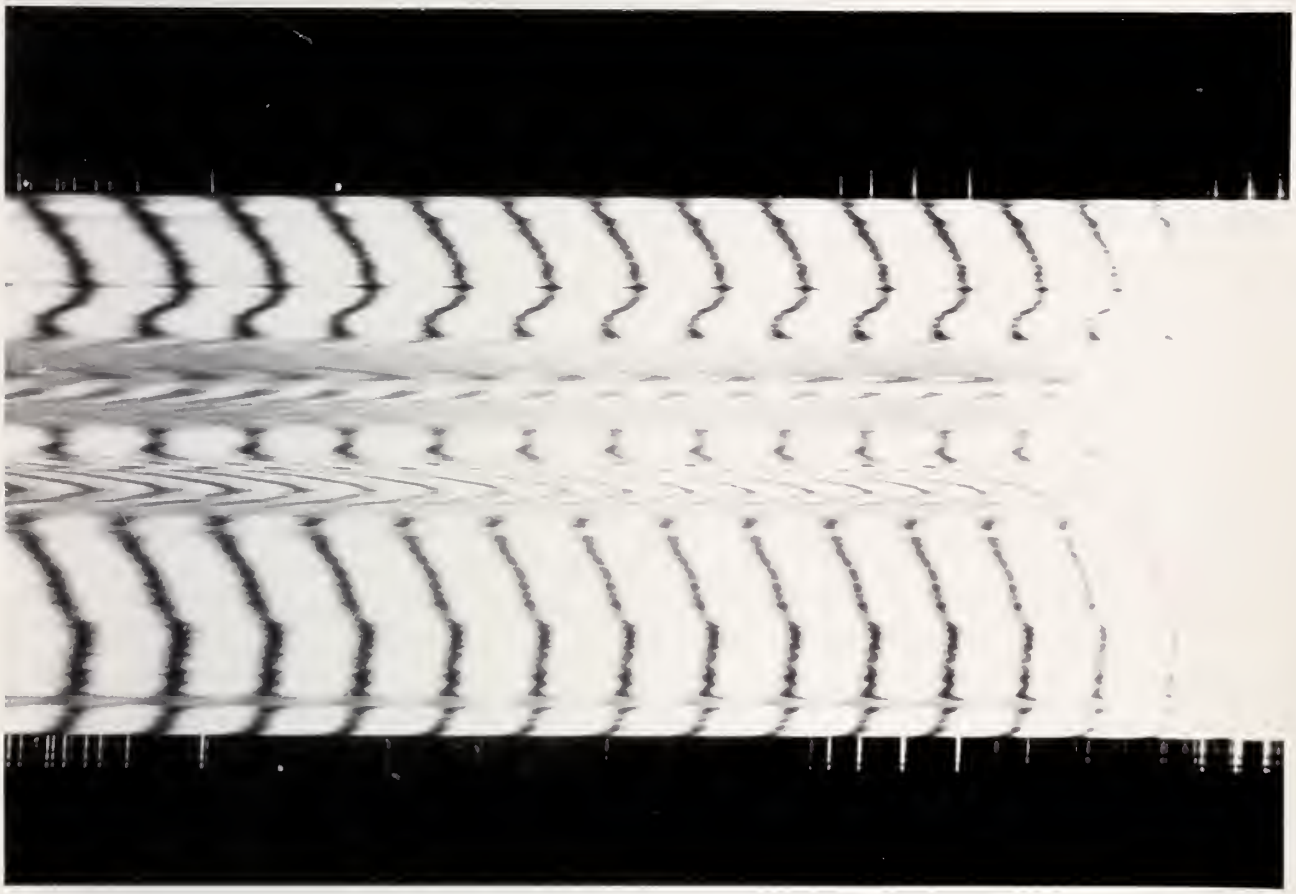

Fig. 10. Fringes of equal chromatic order.
Section GG as in Fig. 8.

of eight profiles based on the fringe patterns, and computed from equation (16).

What may be an interesting feature of the row of etch pits is the small ridge, about a tenth of a micron high, on either side of the pits. Unfortunately, this height is less than the tolerance in the profile measurements.

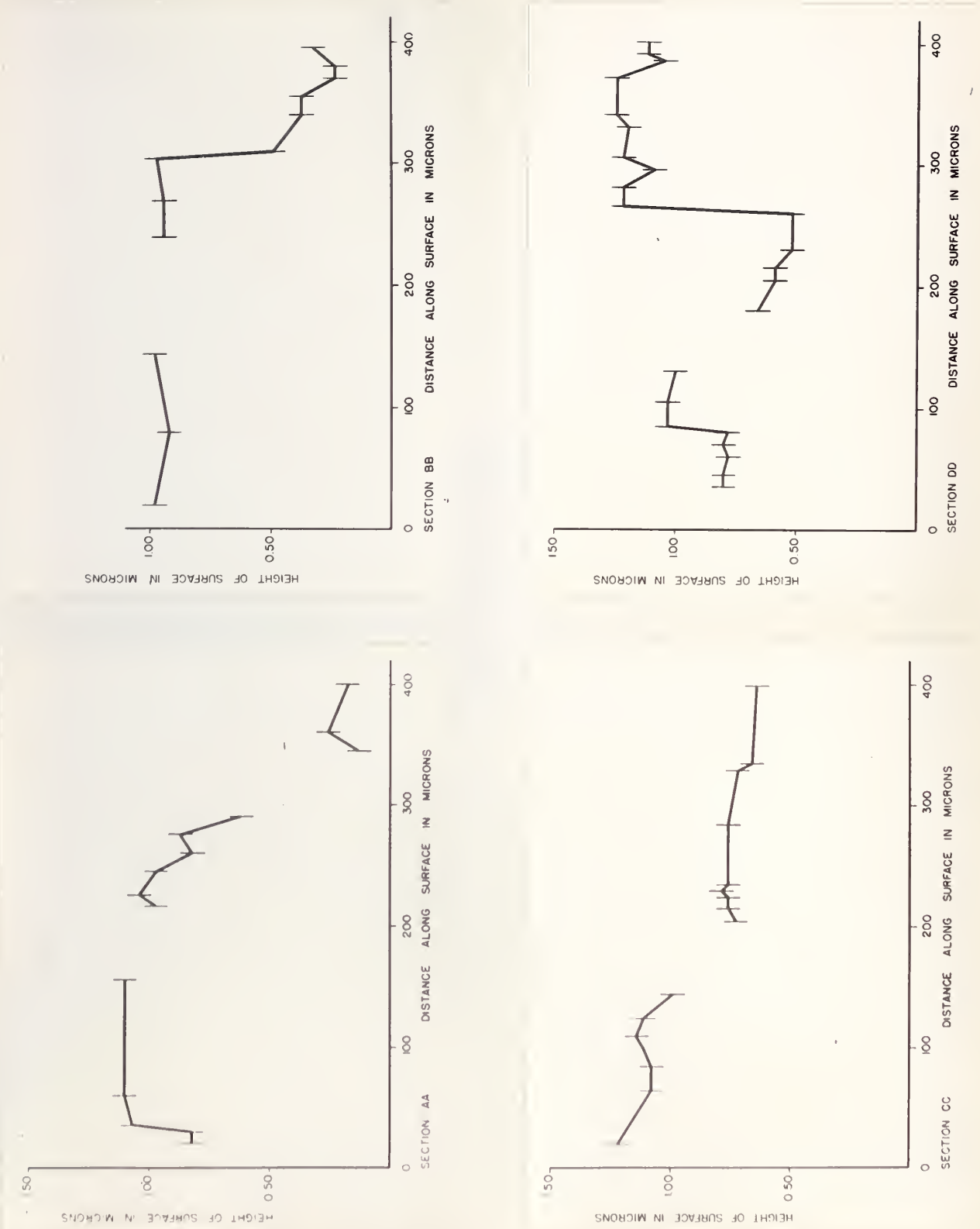


Fig. 11. Set of profiles of the region of Fig. 6 as keyed in Fig. 8.

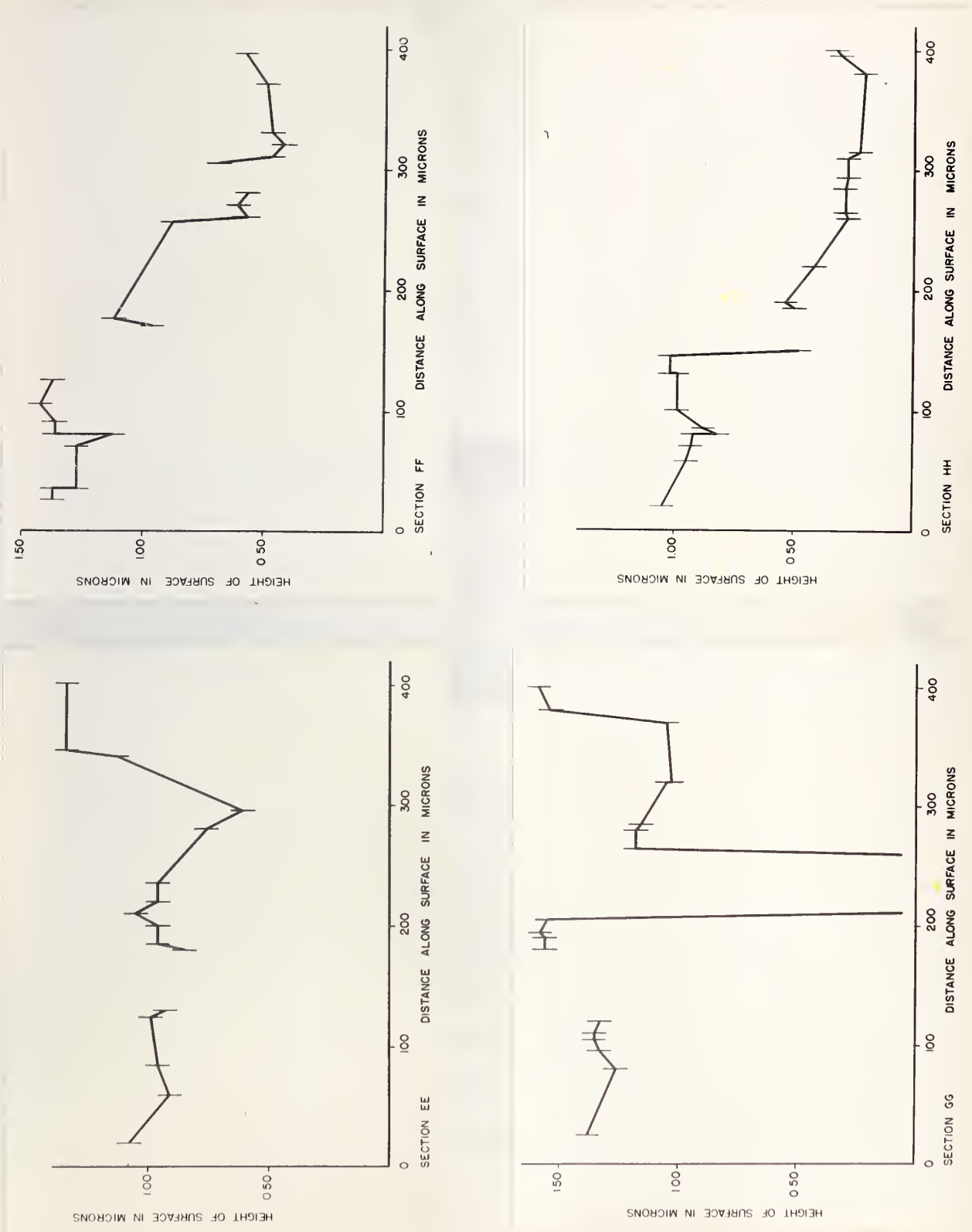


Fig. 11. (Cont.) Set of profiles of the region of Fig. 6 as keyed in Fig. 8.

There are some restrictions on the usefulness of the fringes of equal chromatic order evident from Figs. 9 and 10. Most prominent is the difficulty of following one fringe across the whole width of the spectral band. Furthermore, only a few fringes can be employed. The dispersion of the spectroscope makes the fringes on the violet side too wide, while the greater intensity of the source cuts off the pattern through overexposure on the red side (Fig. 12).

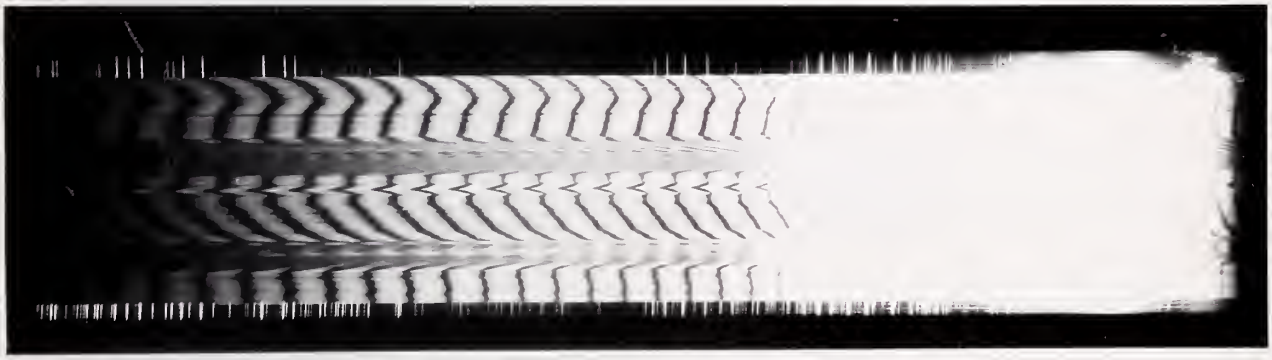

Fig. 12. A complete spectral photograph for section EE showing the narrowness of the usable portion of the spectrum.

Conditions which will produce quite acceptable monochromatic fringes often will not yield good fringes of equal chromatic order. Fig. 13 is a monochromatic contour map of part of a polycrystalline specimen. Fig. 14 shows a band of fringes of equal chromatic order in the same region. They are quite useless. Fig. 15 shows another region of the

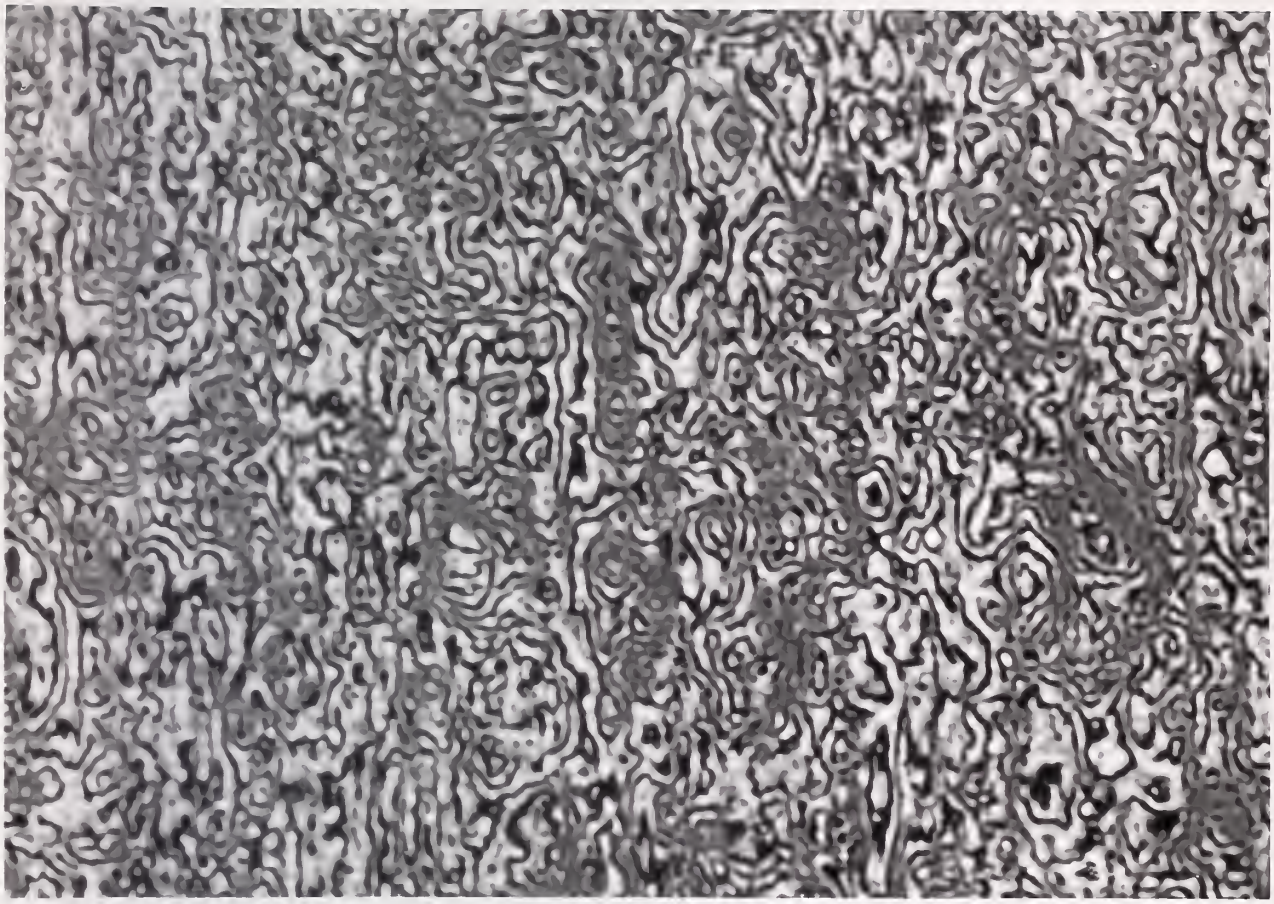

Fig. 13. A monochromatic contour map of a portion of a polycrystalline specimen.

same specimen after a washing with hydrogen peroxide. The surface is thereby made more reflective, and the quality of the fringes of equal chromatic order (Fig. 16) improved. They are still, however, inferior. Furthermore, chemical treatment of this sort cannot be used without introducing extraneous properties onto the surface under examination.

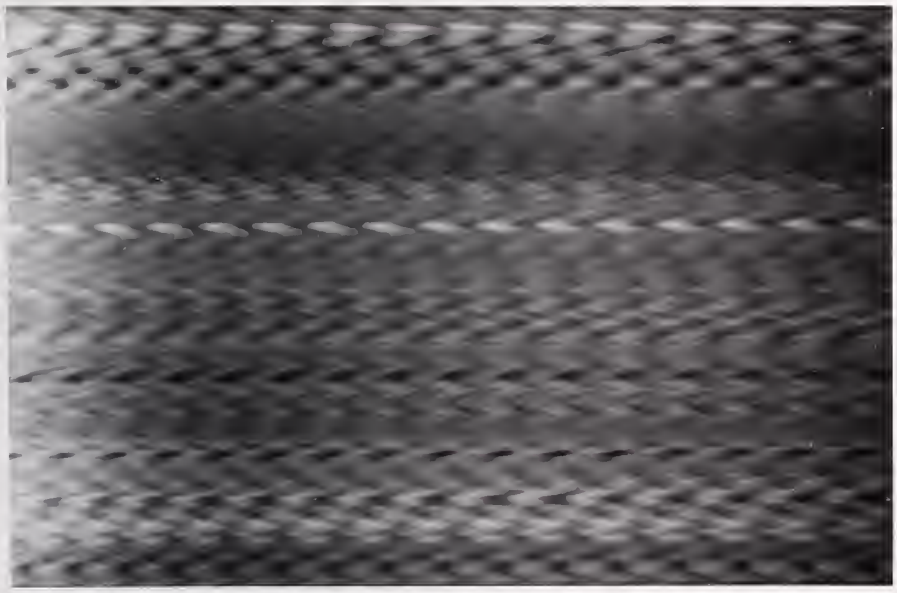

Fig. 14. Fringes of equal chromatic order from the region of Fig. 13.

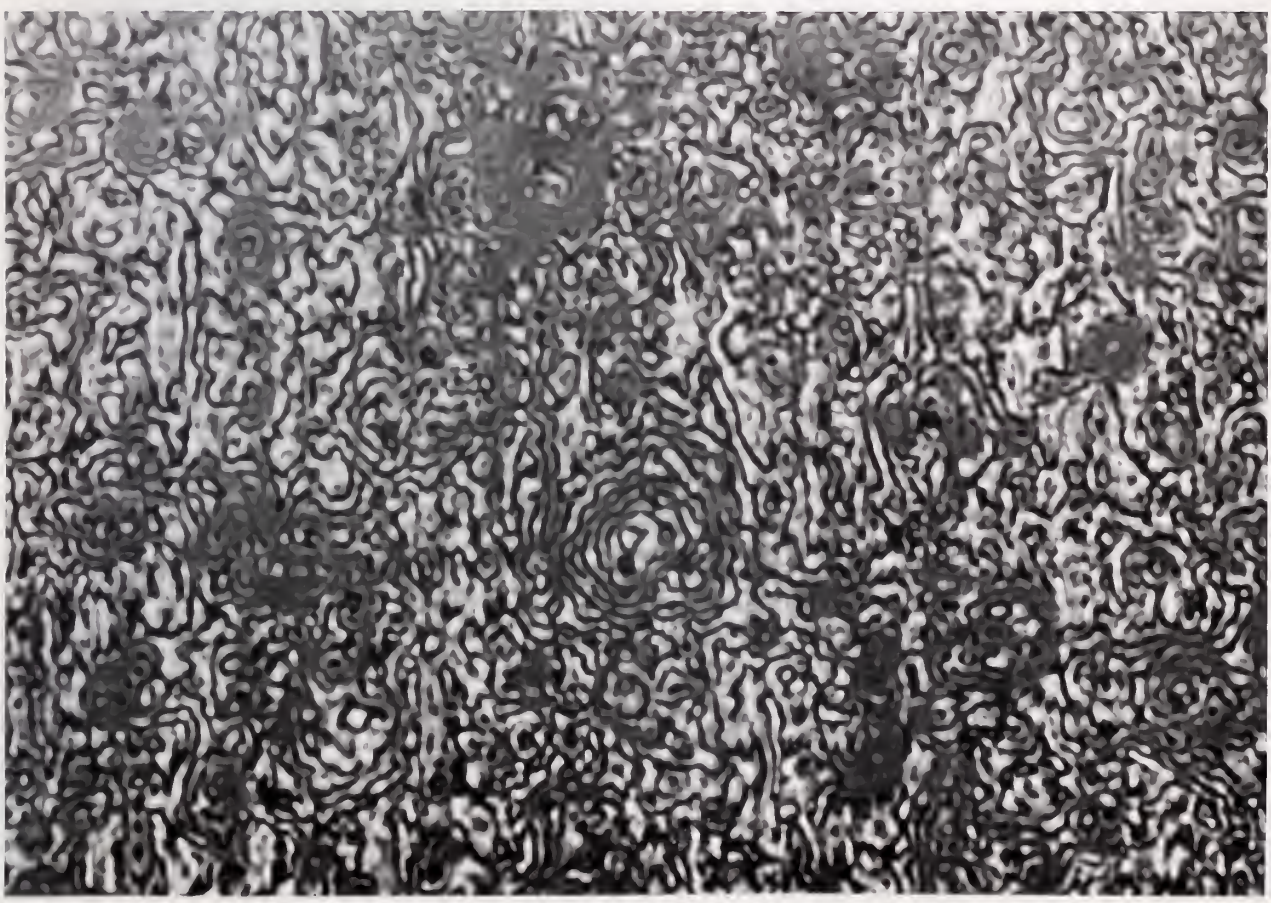

Fig. 15. A monochromatic contour map of a portion of the same polycrystalline specimen as in Fig. 13, after a washing with hydrogen peroxide.

Fig. 16. Fringes of equal chromatic order from the region of Fig. 15.

The fringes of equal chromatic order are seen to possess a fine structure (Fig. 17). When the optical flat was replaced by a fire-polished glass square, the fine structure appeared as in Fig. 18. Tolansky[11] attributes the fine structure to small irregularities in the lenses and flats. Since the fire-polished flat should be free from the traces of the conventional rouge polishing, it appears from Figs. 17 and 18 that the fine structure is due to inhomogeneities in the glass, which would alter slightly the various optical path lengths, rather than to superficial irregularities arising from the polishing.

The monochromatic fringes also may possess a fine

---

11. S. Tolansky, Multiple-Beam Interferometry of Surfaces and Films (Clarendon Press, Oxford, 1948), p. 103.

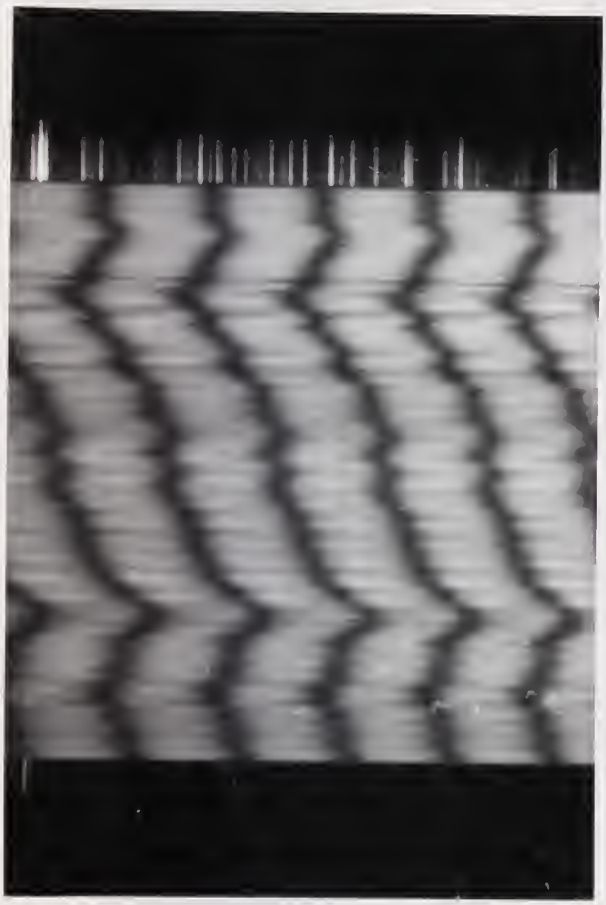

Fig. 17. Fine structure of fringes of equal chromatic order arising from the use of a conventional optical flat.

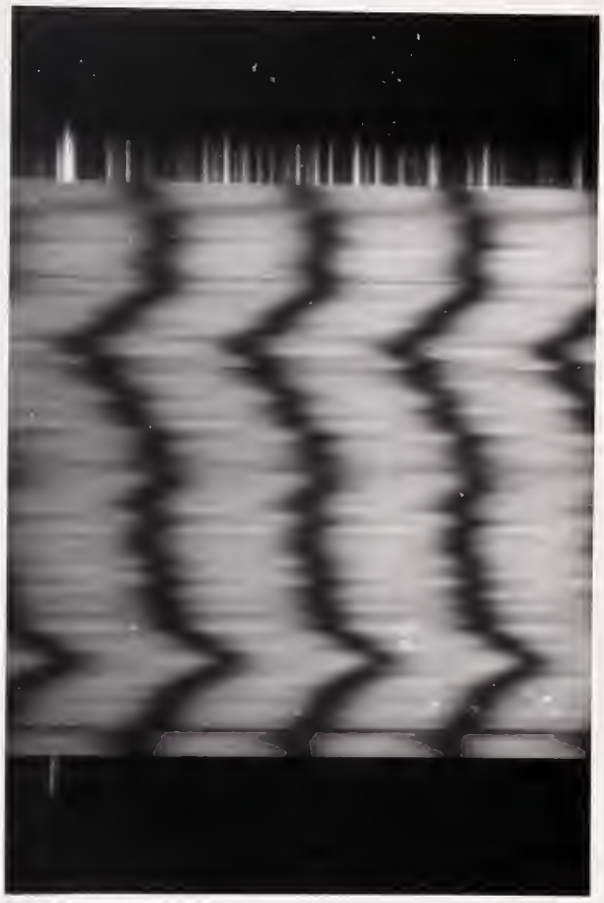

Fig. 18. Fine structure of fringes of equal chromatic order arising from the use of a fire-polished optical flat.

structure. Examination of a polycrystalline specimen revealed the phenomenon of fringe "doubling" (Fig. 19). Tolansky[12] has observed an apparently similar effect, which he ascribes to the phase change upon reflection at the metal surface of non-normally incident light resulting in differently polarized components. By means of a pair of Polaroid filters, the

---

12. S. Tolansky, Multiple-Beam Interferometry of Surfaces and Films (Clarendon Press, Oxford, 1948), p. 38.

Fig. 19. Monochromatic fringes showing the "doubling" effect.

specimen was examined in polarized light, but no circumstances were found which would affect the main fringes which did not also similarly affect the secondary fringes. Fig. 19 is not, therefore, a demonstration of the polarizing effect of metallic reflectors. The specimen was accidentally melted during an annealing process, after which the "doubling" effect was no longer observed, nor has it been observed on any other specimen.

However, a close scrutiny of Fig. 19 shows that the fringes are tripled, in places, on the side toward the center of the small hollow. This is the fine structure discussed by Kinosita[13] from a theoretical standpoint, and, so far as is known, it has not hitherto been observed. It may also be noticed from Fig. 19 that the maxima of intensity occur adjacent to the minima. This type of asymmetry is quite explicable, and has been dealt with by Hamy[14].

0 hours

2 hours

Fig. 20. Monochromatic fringes arising from specimens heated at 400° C for various lengths of time.

---

13. K. Kinosita, J. Phys. Soc. Japan 8, 219 (1953).

14. M. Hamy, J. de Phys. 5, 793 (1906).

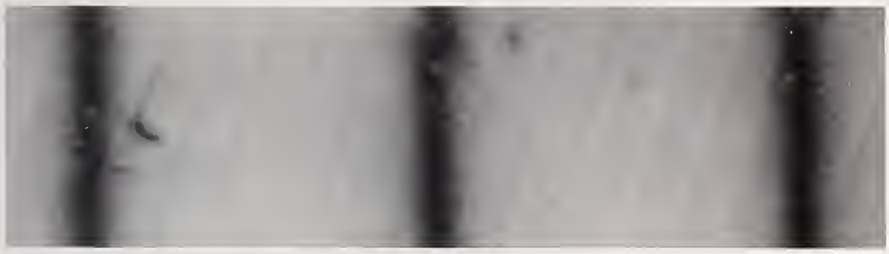

4 hours

6 hours

12 hours

18 hours

Fig. 20 (Cont.) Monochromatic fringes arising from specimens heated at 400° C for various lengths of time.

Fig. 20 shows the appearance of monochromatic fringes formed with specimens consisting of microscope slides coated with aluminum, and maintained at 400° C for various lengths of time. The fringes are broader for the longer times of heating, which correspond to the thicker oxide coatings. This is to be expected from the theory (p. 6), since the thicker oxide will mean a longer path difference for the non-dominant beams, which will result in greater phase differences to detract from the sharpness of the fringes.

The sharpness of the fringes also depends on the number of beams contributing to the multiple-beam interference. In all the cases encountered in these experiments, with the single exception of that illustrated by Fig. 20, the best fringes were produced by use of a dielectric coated optical flat with a reflectivity of 0.43 for mercury green light. The coated slides enabled a flat of reflectivity 0.71 to be used for the photographs in Fig. 20. Williams[15] cites a quantity, "the effective number of multiple beams," based on resolving power considerations, and specified in terms of the mean reflectivity of the interferometer surfaces. If, as an approximation, the reflectivity of the flat is taken to be the mean reflectivity, it is found that for the 0.43 reflective flat, there are 3.0 effective beams, while for

---

15. W.E. Williams, Applications of Interferometry (Methuen, London, 1928), p. 80.

the 0.71 there are 7.5. Williams alludes to unpublished work by Hansen which, in the examples cited by Williams, shows that Williams' estimates are about fifteen percent too low. So these values should be regarded only as giving the order of magnitude of the number of effective beams.

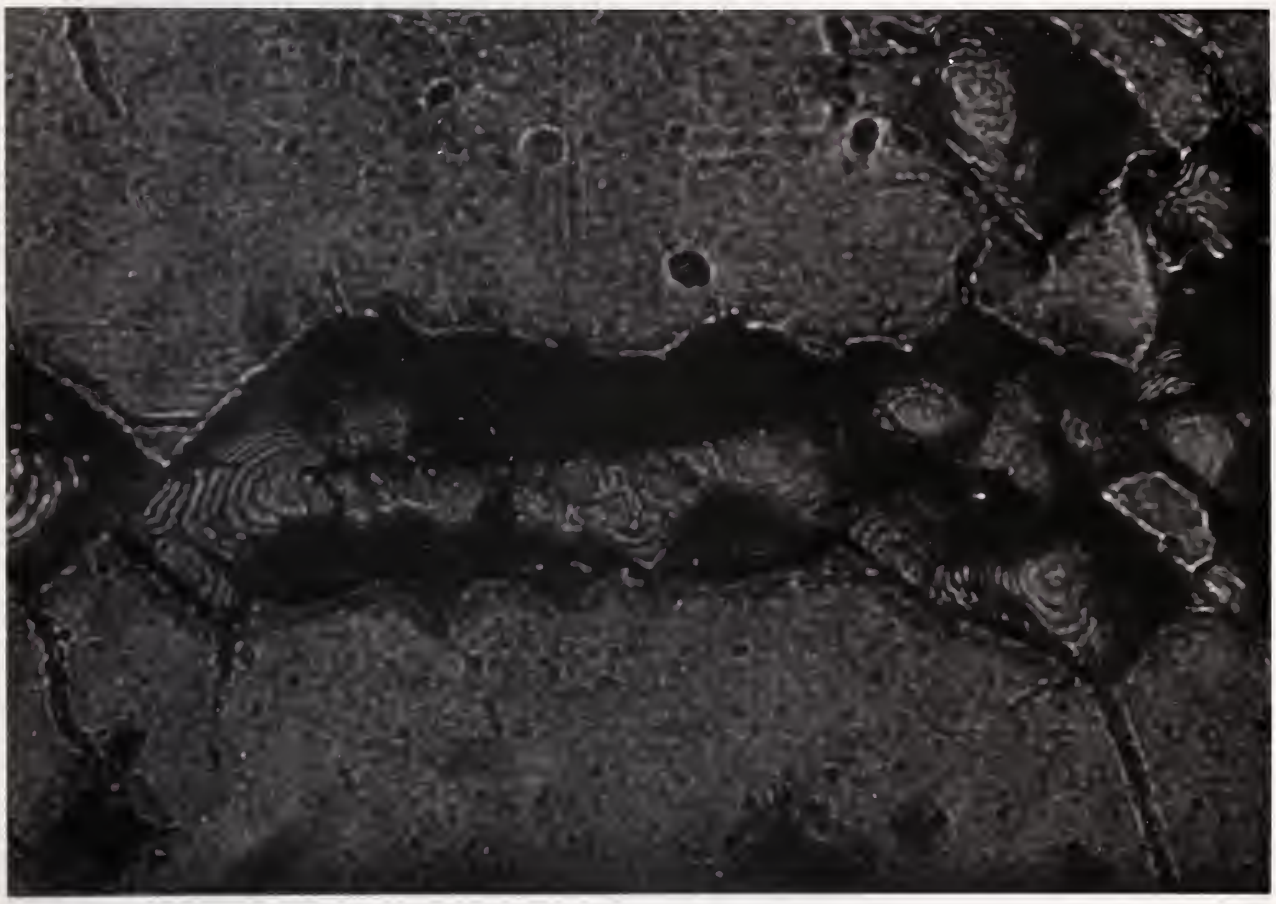

Fig. 21. Monochromatic fringes arising from the presence of a film of monobromonaphthalene instead of an optical flat.

Fig. 21 illustrates a likely explanation of the

interference fringes occasionally seen without the use of an optical flat. A few drops of monobromonaphthalene, which has an index of refraction of 1.66, which is fairly close to that of aluminum oxide, 1.765, were placed on the specimen. The tops of these drops acted like the partially reflecting surface of a flat. Thus the appearance of fringes without any flat is likely due to an unusually thick local deposit of aluminum oxide.

## VI. Discussion

The use of multiple-beam interference fringes in metallographic studies of aluminum appears definitely practicable. Although the monochromatic fringes give a good qualitative impression of the nature of the surface, it is the fringes of equal chromatic order which provide the tool for detailed study of surface characteristics. Other metals which have oxide coatings might also be examined by this technique, provided that their reflectivities are sufficiently high to enable the fringes of equal chromatic order to be formed.

The principal limitations on the use of the multiple-beam fringes seem to be the comparative narrowness of the usable portion of the spectrum of fringes of equal chromatic order, and the need for specially prepared surfaces. Some improvement in the former case might be brought about by the use of special photographic materials which would allow more of the red end of the spectrum to be used; the broadening of the fringes caused by the dispersion of the spectroscope and the long exposures necessitated by the feeble illumination at the violet end of the spectrum make extension of the usable band of fringes into that spectral region unpromising. The need for specially prepared surfaces prevents the examination

of interesting conditions which arise during processes which may only incidentally lower the reflectivity of the surface, e.g. corrosion. This problem might be overcome by vacuum plating of the surface with silver, which Tolansky[16] has shown will contour very closely the surface so coated.

It is the presence of the oxide film on the surface of the aluminum which makes the study of that metal more complex than that of gold, say. The varying widths of the monochromatic fringes (Fig. 7) indicate that the oxide thickness is not uniform. This failure of the oxide coating to contour the surface exactly is further demonstrated by the occurrence of fringes without the use of an optical flat, which has been seen to indicate the presence of a thick layer of oxide. These same broadenings of the fringes prevent the use of Brossel's[17] ingenious method of telling the sense of the gradients by examination of the asymmetrical shape of the monochromatic fringes, the more gradual decrease in intensity indicating a descent away from the flat.

Tolansky[18] employs very close contacts between the surface being examined and the optical flat. This enables him to use much lower orders of interference in the fringes of equal chromatic order with the resulting increased spacing of the

---

16. S. Tolansky, Multiple-Beam Interferometry of Surfaces and Films (Clarendon Press, Oxford, 1948), p. 63.

17. J. Brossel, Nature 157, 623 (1947).

18. S. Tolansky, op. cit., p. 99.

fringes and the consequent decrease in the relative error in determining the wavelength at which the fringes occur. The presence of the oxide layer of variable thickness prevents the use of close contacts since the optical path must be related to the profile distance by equation (9). If $s_{23}$ is not negligible compared to $s_{12}$, then $s_{23}$ must be known in order to find $\mu$, which will no longer be very close to $\mu_{12}$. Knowledge of the oxide thickness is difficult to obtain, especially since it would have to be measured on a very small region of the surface due to the variability of the thickness within distances along the surface the order of ten microns.

It is perhaps surprising that the method yields the results it does, despite the high order of interference employed and the low number of effective beams interfering. Nevertheless, the technique should provide metallography with a useful complement to the modern two-beam interference microscope, for which the spectroscopic examination of fringes, emphasized here, is unsuitable.

## Bibliography

General

S. Tolansky, Multiple-Beam Interferometry of Surfaces and Films (Clarendon Press, Oxford, 1948).

B. Chalmers and W.E. Hoare, "Metallography: a New Technique," Nature 141, 475 (1938).

Interference Theory

R.L. Mooney, "An Exact Theoretical Treatment of Reflection-Reducing Optical Coatings," J. Opt. Soc. Am. 35, 574 (1945).

G.H. Hardy and E.M. Wright, An Introduction to the Theory of Numbers (Clarendon Press, Oxford, 1938).

W.F. Koehler, "Multiple-Beam Fringes of Equal Chromatic Order. Part I. Phase Change Considerations," J. Opt. Soc. Am. 43, 738 (1953).

Aluminum Oxide

Handbook of Chemistry and Physics (Chemical Rubber Publishing Company, Cleveland, 1953), thirty-fifth edition.

G.D. Scott, "Optical Constants of Thin-Film Materials," J. Opt. Soc. Am. 45, 179 (1955).

J.C. Slater and N.H. Frank, Electromagnetism (McGraw-Hill Book Company, Inc., New York, 1947).

O. Kubaschewski and B.E. Hopkins, Oxidation of Metals and Alloys (Butterworth Scientific Publications, London, 1954).

W.W. Smeltzer, "Review of the Literature on Oxide Films on Metals with Special Reference to Aluminium," Aluminium Laboratories Limited Report No. K-RR-450-54-28 (Kingston, 1954).

Fringe Shape

M. Hamy, "Sur le Franges de Réflexion des Lames Argentées," J. de Phys. 5, 793 (1906).

J. Brossel, "Asymmetrical Broadening with Multiple-Beam Interference Fringes," Nature 157, 623 (1946).

K. Kinosita, "Numerical Evaluation of the Intensity Curve of a Multiple-Beam Fizeau Fringe," J. Phys. Soc. Japan 8, 219 (1953).

W.E. Williams, Applications of Interferometry (Methuen, London, 1928).

## Appendix I

## Calibration of Wavelength Scale

The lines of the iron arc spectrum were identified from the tables[19] (Fig. 22), and a dispersion curve for the constant deviation spectroscope plotted (Fig. 23).

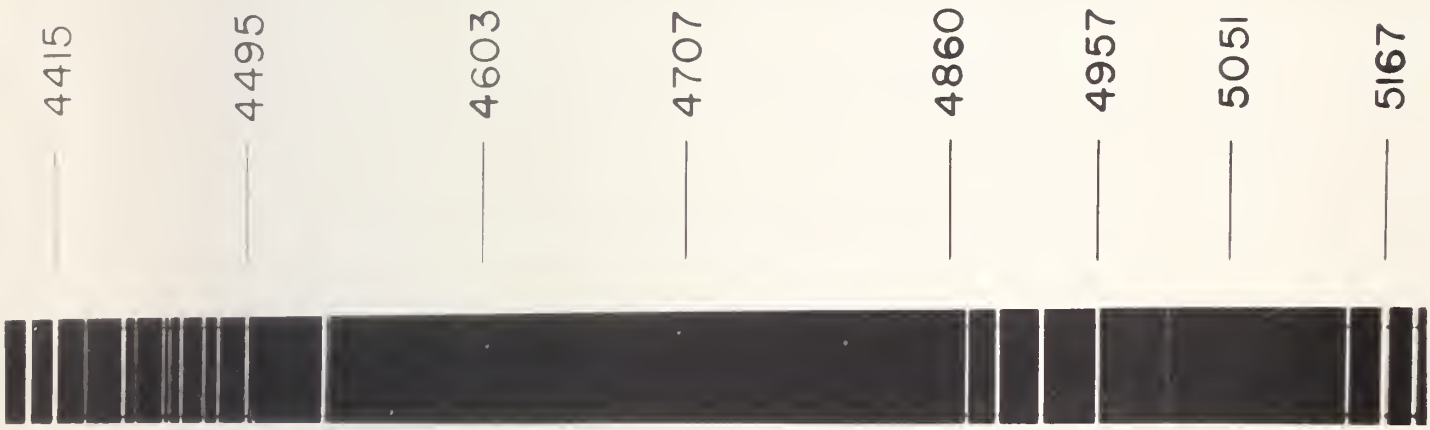


Fig. 22. Spectrum of the iron arc.

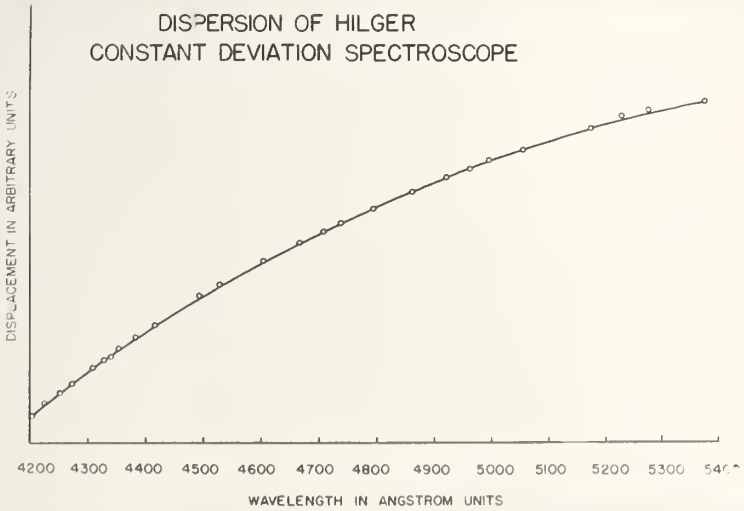


Fig. 23. Dispersion curve used to construct a wavelength scale.

---

19. Handbook of Chemistry and Physics (Chemical Rubber Publishing Company, Cleveland, 1953), thirty-fifth edition, p. 2535 - 2537.

The axis of ordinates of this curve was the basis on which a master wavelength scale, suitable for a variety of enlargement sizes, was constructed (Fig. 24).

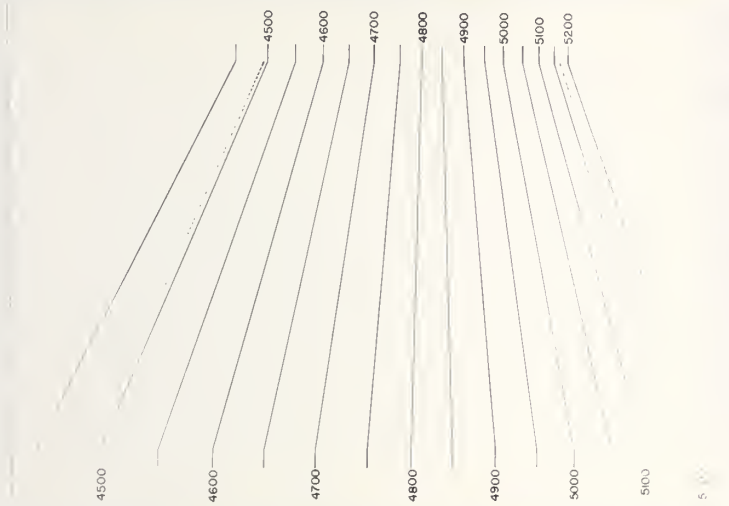


Fig. 24. Master wavelength scale.

## Appendix II

## Photoelectric Exposure Meter

Fig. 25 shows the circuit of a sensitive photoelectric exposure meter capable of measuring illumination at very low levels. Details of the power supply, which is quite conventional, are not shown since the power supply was obtained as a completed unit. The sensitivity is illustrated by the fact that a reading of 7.5 (full scale, 50.0) means a ten minute exposure on Pan F film (ASA 16).

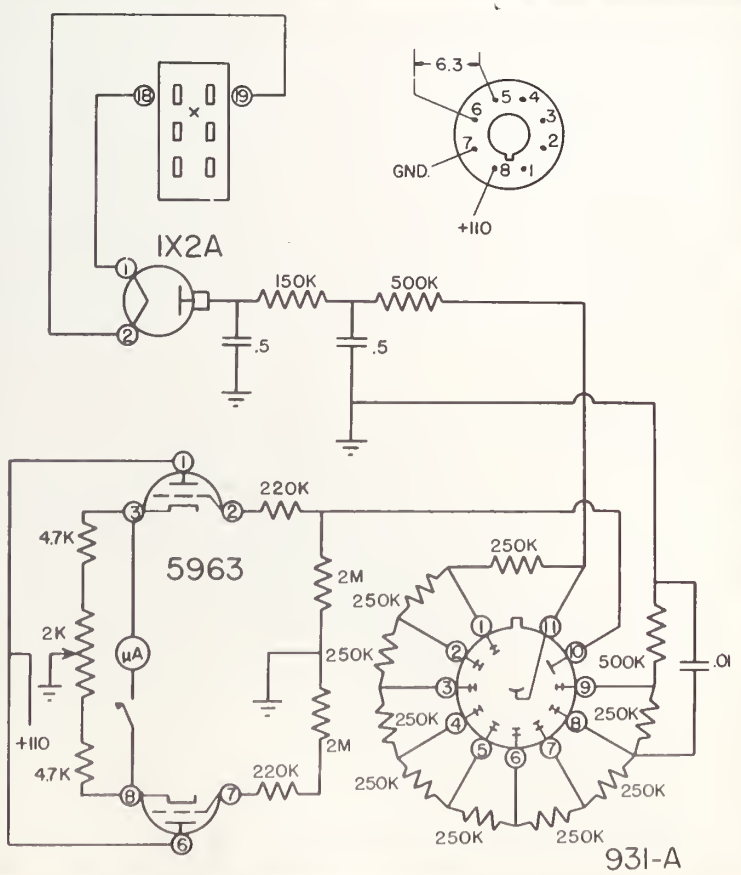


Fig. 25. A sensitive photoelectric exposure meter. All resistances in ohms, capacitances in microfarads, potentials and potential differences in volts.

## Appendix III

## Study of Surface Anomalies

The disturbing effect of the oxide film in studying the surface topography of a metal will be most pronounced near a marked local anomaly such as an etch pit. Etch pits are particularly valuable since they may also be used to reveal the underlying crystallographic orientation. A further advantage of etch pits is that it is possible to manufacture them where they are wanted.

If the oxide layer varies in thickness over the bottom of an etch pit, the appearance of the bottom will be distorted by the refraction of the light passing through the surface of the oxide. Fig. 7 (p. 19) shows how the oxide may obscure the topography of the pits. It may however happen that the pits are not obscured (Fig. 26), but such an event is fortuitous.

The specimen shown in Fig. 26 was electropolished[20] in an electrolyte[21] containing 40%wt $H_2SO_4$, 40%wt $H_3PO_4$, and 20%wt $H_2O$. A brass cathode was used, and polishing continued until clouds of greenish-black material began forming in the electrolyte.

---

20. George L. Kehl, The Principles of Metallographic Laboratory Practice (McGraw-Hill Book Company, Inc., New York, 1943), second edition, p. 19.

21. S.J. Basinska, J.J. Polling, and A. Charlesby, Acta Met. 2, 313 (1954).

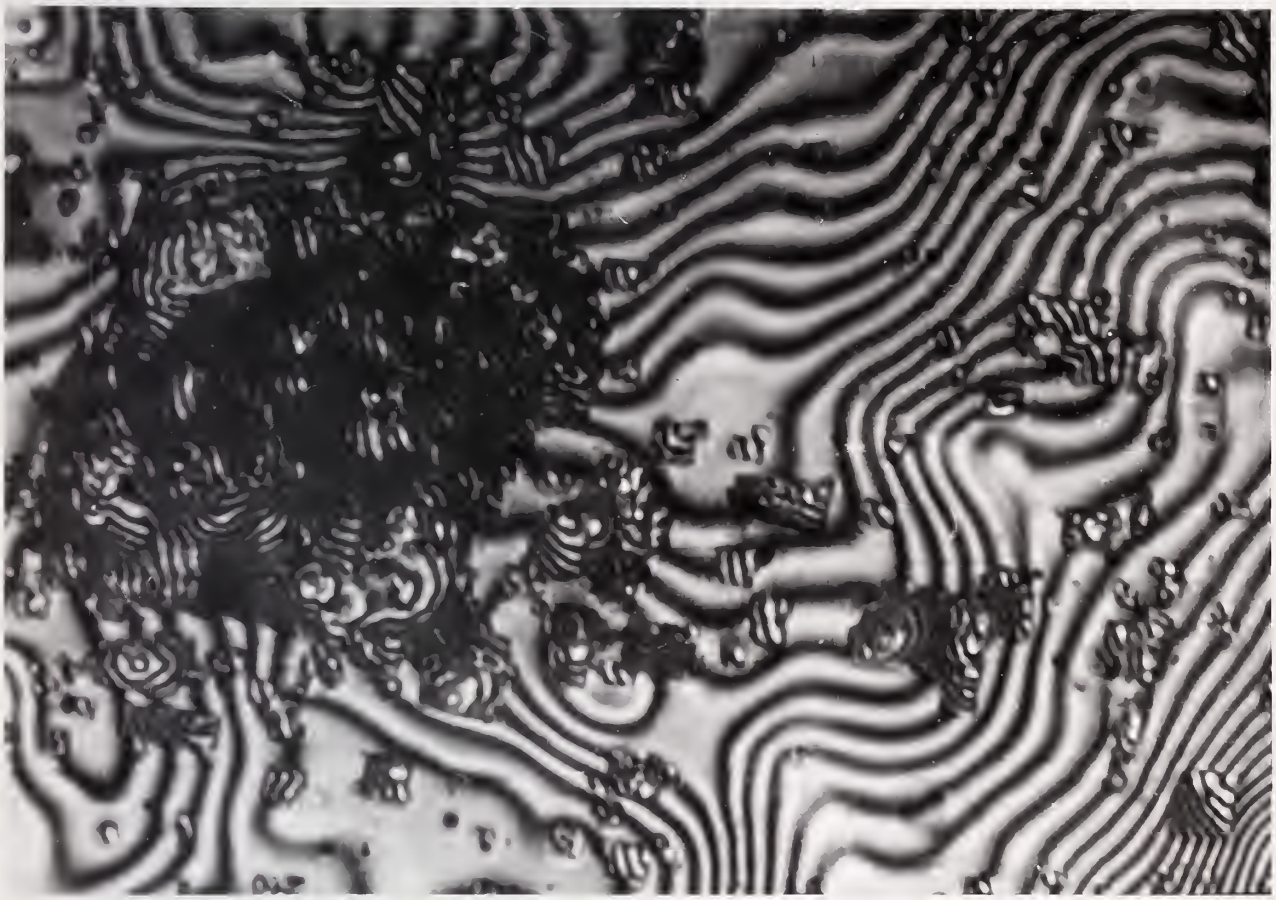

Fig. 26. An etched polycrystalline specimen showing the formation of etch pits.

The etchant employed consisted of 9 parts HCl, 3 parts $HNO_3$, 2 parts HF, and 5 parts $H_2O$[22]. The specimen was set in a block of ice and the etchant applied. The etching was done for two minute periods at the end of each of which the specimen was examined interferometrically.

---

22. Charles S. Barrett, Structure of Metals (McGraw-Hill Book Company, Inc., New York, 1943), p. 175.